

This article was downloaded by: [University of California, San Diego]

On: 07 August 2012, At: 12:23

Publisher: Taylor & Francis

Informa Ltd Registered in England and Wales Registered Number: 1072954 Registered office: Mortimer House, 37-41 Mortimer Street, London W1T 3JH, UK



## Molecular Crystals and Liquid Crystals

Publication details, including instructions for authors and subscription information:

<http://www.tandfonline.com/loi/gmcl20>

### Electric Field Induced Orientational Order in Suspensions of Anisotropic Nanoparticles

Robert Greasty<sup>a</sup>, Jana Heuer<sup>b</sup>, Susanne Klein<sup>b</sup>, Claire Pizzey<sup>c</sup> & Robert Richardson<sup>a</sup>

<sup>a</sup> H H Wills Physics Laboratory, University of Bristol, United Kingdom

<sup>b</sup> HP Laboratories, Stoke Gifford, Bristol, United Kingdom

<sup>c</sup> Diamond Light Source Ltd, Diamond House, Didcot, United Kingdom

Version of record first published: 30 Jun 2011

To cite this article: Robert Greasty, Jana Heuer, Susanne Klein, Claire Pizzey & Robert Richardson (2011): Electric Field Induced Orientational Order in Suspensions of Anisotropic Nanoparticles, *Molecular Crystals and Liquid Crystals*, 545:1, 133/[1357]-145/[1369]

To link to this article: <http://dx.doi.org/10.1080/15421406.2011.568888>

PLEASE SCROLL DOWN FOR ARTICLE

Full terms and conditions of use: <http://www.tandfonline.com/page/terms-and-conditions>

This article may be used for research, teaching, and private study purposes. Any substantial or systematic reproduction, redistribution, reselling, loan, sub-licensing, systematic supply, or distribution in any form to anyone is expressly forbidden.

The publisher does not give any warranty express or implied or make any representation that the contents will be complete or accurate or up to date. The accuracy of any instructions, formulae, and drug doses should be independently verified with primary sources. The publisher shall not be liable for any loss, actions, claims, proceedings, demand, or costs or damages whatsoever or howsoever caused arising directly or indirectly in connection with or arising out of the use of this material.

# Electric Field Induced Orientational Order in Suspensions of Anisotropic Nanoparticles

ROBERT GREASTY,<sup>1</sup> JANA HEUER,<sup>2</sup>  
SUSANNE KLEIN,<sup>2</sup> CLAIRE PIZZEY,<sup>3</sup> AND  
ROBERT RICHARDSON<sup>1</sup>

<sup>1</sup>H H Wills Physics Laboratory, University of Bristol, United Kingdom

<sup>2</sup>HP Laboratories, Stoke Gifford, Bristol, United Kingdom

<sup>3</sup>Diamond Light Source Ltd, Diamond House, Didcot, United Kingdom

*Suspensions of anisometric dye particles in dodecane have been investigated by electro-optic methods and X-ray scattering. The suspensions have nematic like properties such as a Schlieren texture and an electro-optic response. The thin, plate-like, particles of Permanent Rubine are crystalline monodomains with a set of lattice planes spaced by 18 Å lying parallel to their largest faces. They are oriented by an electric field such that their normals tend to be perpendicular to the applied field. The stronger ordering at about 25 wt% suggests that this might be the onset of the nematic phase. A simple model shows that the electric field induced change in optical absorbance is consistent with the induced orientational order.*

**Keywords** Anisotropic nanoparticle suspension; electric field ordering; orientational order; X-ray scattering

## 1. Introduction

Smart colloids, that is colloids which respond to applied fields, are interesting for many applications reaching from security printing to electronic paper. The electronic paper, commercially available in e-readers, is based on electrophoresis which, in its present embodiment, does not give a light-efficient full colour display. To achieve colour for a reflective display we are looking into pigment suspensions which react to an applied electric field with a change of hue. The reorientations of anisotropic colloidal particles in suspension have been observed before, however all these systems previously studied are transparent and do not show any colour effects. Thus the motivation for this work is different from the fundamental studies of model systems of anisotropic particles, which are not coloured [1–3].

---

Address correspondence to Robert Richardson, H H Wills Physics Laboratory, University of Bristol, United Kingdom. Tel.: +44 (0)117 928 7666; Fax: +44 (0)117 9255624; E-mail: robert.richardson@bristol.ac.uk

## 2. Experimental

### 2.1. Suspensions

As a test particle we use C.I. Pigment Red 57:1 [4]. It is commercially available as Permanent Rubine L4B01 from Clariant (used as received) where the primary particles are rectangular platelets with the chemical formula shown in Figure 1(a). The particles have a mean width of 131 nm (17 nm), a length of 280 nm (230 nm) and a thickness of 10 nm (5 nm) where the second value is an indication of the range. The particles are very polydispersed, as shown in Figure 1(b), but when they are suspended in dodecane using the commercially available dispersant Solsperse 11200 (Lubrizol, used as received) they show optical effects similar to low molecular weight thermotropic liquid crystals.

Depending on the pigment concentration the suspensions show several different effects. At low concentrations (<10 wt%) the suspension seems to be homogenous between glass substrates, but when a field is applied we can observe reversible phase separation. For concentrations between 10 wt% and 30 wt% certain fields can lead to electroconvection or just to a change in tone. From 35 wt% upwards the suspension is so viscous that Schlieren textures forming around air bubbles or at any air/suspension interface become permanent (Figure 2).

We will focus here on a combination of pigment concentrations and electric fields which lead to a hue change only, avoiding phase separation and electro-convection.

### 2.2. Optical Measurements

To measure the absorbance of the suspension as a function of applied electric field the suspensions were capillary filled into 5 micron Indium Tin Oxide (ITO) glass

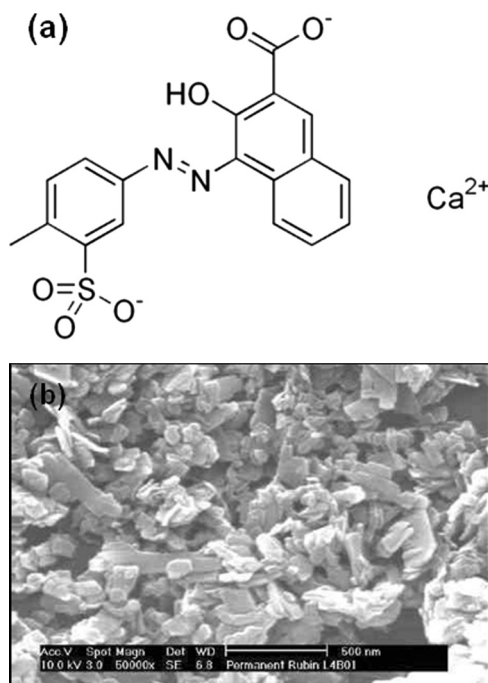


**Figure 1.** (a) Chemical formula and (b) SEM of Permanent Rubine L4B01.

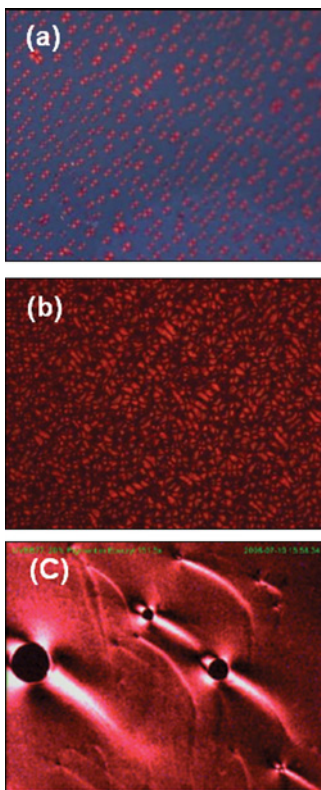


**Figure 2.** Suspension between crossed polarisers; (a) reversible phase separation, (b) electro-convection and (c) Schlieren texture. (Figure appears in color online.)

cells. The substrates had a flat ITO layer covered with rubbed polyimide. The samples were placed on the stage of a Zeiss Axiolab polarisation microscope where the eye piece was replaced by an Ocean Optics spectrometer. The electric field lines were in the same direction as the illumination. Permanent Rubine has a well defined absorption peak between 500–600 nm as shown in Figure 3(a).

For concentrations between 1 wt% and 35 wt% the absorption peak decreased with increasing field (1 kHz, square wave) as shown in Figure 3. At the peak, the absorbance ratio between  $0.2 \text{ V}/\mu\text{m}$  field and  $8 \text{ V}/\mu\text{m}$  was about  $1.3 \pm 0.1$  for the concentrations shown in Figure 4. For concentrations above 20 wt% the measurements were not accurate because of the very high absorption. However, the same ratio was determined at the edge of the peak (400 to 490 nm) where the absorption was less for concentrations up to 35 wt%. The suspension showed flow alignment, but no surface alignment with the substrate surface. It was therefore not surprising that we could not observe a Fredericks transition.

### 2.3. X-ray Measurements

Experiments were carried out using the Small Angle X-ray Scattering instrumentation at the I22 beam line at the Diamond Light Source [5]. The experimental setup is shown in Figure 5. Samples ranging in concentration from 1 to 35 wt% were placed

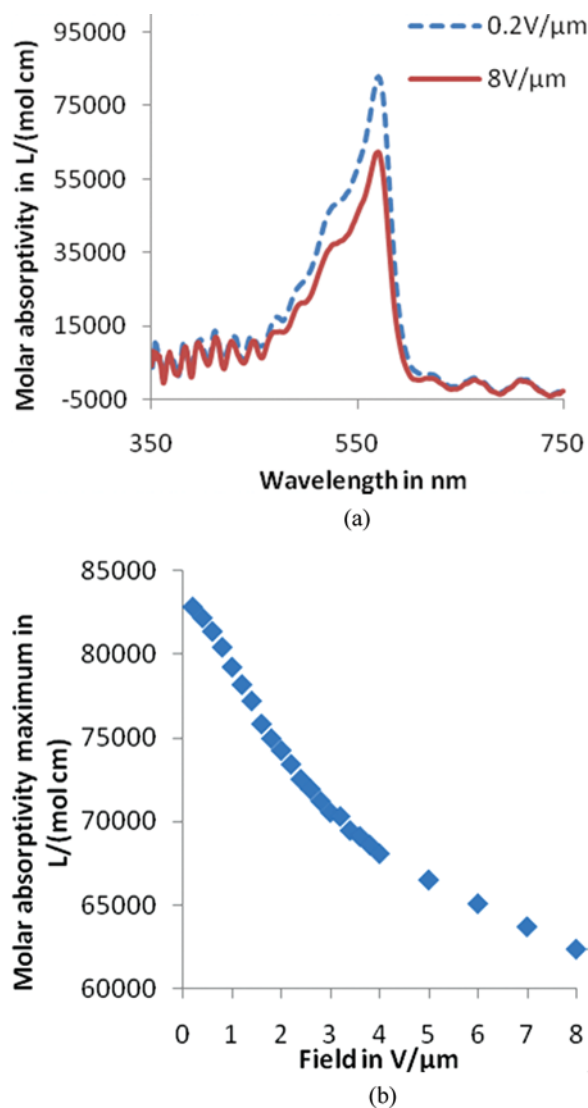


**Figure 3.** Optical results measured for Permanent Rubine in dodecane (5 wt%) (a) Absorption spectrum at 0.2 V/μm and 8 V/μm (b) Absorption maximum as a function of applied field. (Figure appears in color online.)

into 1.5 mm diameter Lindemann glass tubes. A monochromatic beam was incident onto the sample and the scattering pattern was recorded on a two dimensional detector. Electrodes were placed either side of the sample applying an electric field sweep from 0 to 4.25 V/μm.

#### 2.4. X-ray Data Analysis

Two main experiments were conducted using a short camera length (1 m) and a longer camera length (5 m). The short camera length was used to determine the Bragg diffraction peaks from the internal crystal planes of the nanoparticles as shown in Figure 6.

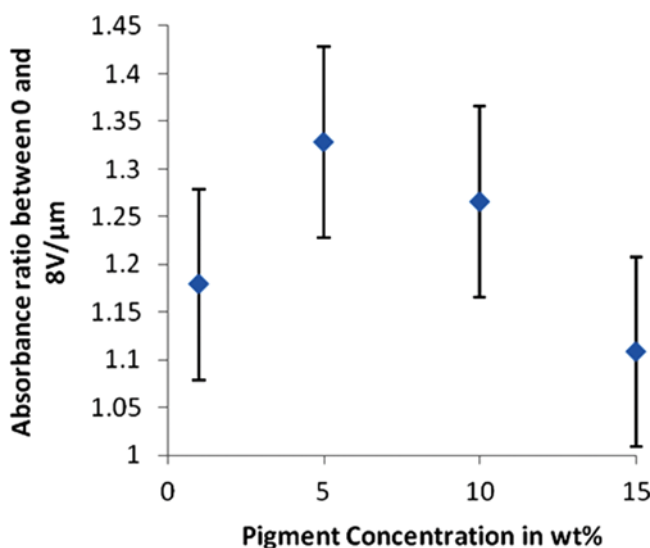


**Figure 4.** Display Dichroic ratio at 570 nm as function of pigment concentration. (Figure appears in color online.)

Figure 6(a) shows a diffraction peak at a scattering vector,  $Q$  of  $0.35 \text{ \AA}^{-1}$  corresponding to a layer spacing of  $18 \text{ \AA}$ . This has been used for orientational order analysis of the particles with applied electric fields. When no field is applied the diffraction peak is isotropically distributed because the lattice planes are randomly orientated. The diffracted rays form the well-known Debye-Scherrer cones which appear on the two dimensional detector as a series of rings. As the electric field is applied the particles reorient so lattice planes align parallel to the field and the diffraction peak becomes anisotropic (Fig. 6(b)). This allows the degree of electro-induced order to be determined [6–9].

The Scherrer formula (Eq. (1)) can be used to relate the radial width of a Bragg peak to the size of the particle [10].

$$\Delta Q = \frac{5.57}{L} \quad (1)$$

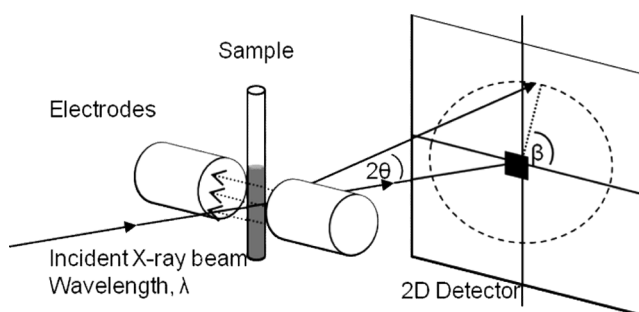


**Figure 5.** The geometry of X-ray scattering experiment from samples with applied electric field.

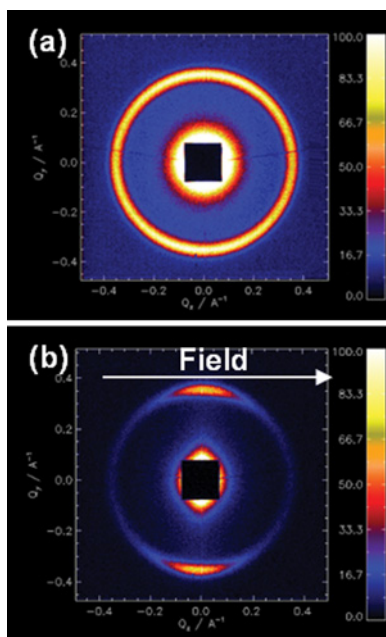


**Figure 6.** Scattering pattern obtained from Permanent Rubine in dodecane (30 wt%) using short camera length with (a) zero field (b) Electric field applied ( $4 \text{ V}/\mu\text{m}$ ). (Figure appears in color online.)

The full width half maximum,  $\Delta Q$ , of the diffraction peak at  $Q = 0.35 \text{ \AA}^{-1}$  has been used to determine the particle size,  $L$ , in a direction perpendicular to the lattice planes. A dimension of  $\sim 12 \text{ nm}$  has been determined indicating that the lattice planes giving the peak at  $0.35 \text{ \AA}^{-1}$  are perpendicular to the thin dimension of the particle. This suggests that the particles are monodomain crystals and their thin dimension tends to align perpendicular to the electric field.

Figure 6 also contains information from the particle form scattering which is partly obscured by the square beam stop protecting the detector. Therefore the particle form scatter was measured separately using a longer camera length and typical data are shown in Figure 7.

Due to the polydispersity of this system the size and shape cannot be determined accurately from particle form scattering. However, the particle form scattering does allow the mean direction of orientation of the platelets to be determined as the scattering is more extended in a direction perpendicular to the direction of the field. This confirms that the small dimension tends to align perpendicular to the direction of the applied electric field.

The X-ray data indicates that both the  $18 \text{ \AA}$  lattice planes and the large dimension of the particles align parallel to the applied electric field as shown in Figure 8. It is reasonable to assume that lattice plane normals  $\mathbf{r}$  are uniaxially distributed with no preference around the applied electric field direction. This means that the degree of alignment of the lattice plane normals  $\mathbf{r}$  to the electric field can be determined by calculating the order parameter of the Bragg scattering peak which directly translates to the order parameter of the particles. This is calculated by dividing the intensity of the Bragg ring into 200 data bins; each one is then integrated and a background, estimated from a nearby part of the detector, removed. The integrated intensity of each

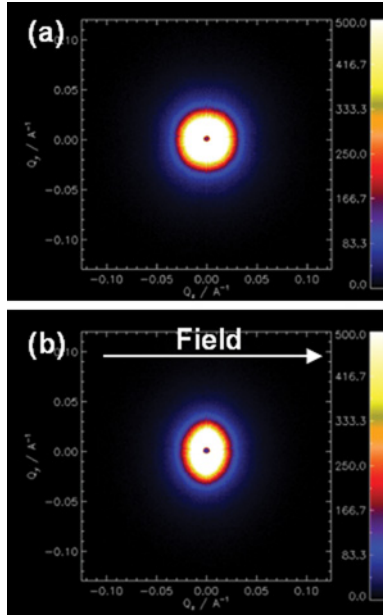


**Figure 7.** Scattering pattern obtained from Permanent Rubine in dodecane (30 wt%) using long camera length with (a) Zero field (b) Electric field applied (4.25 V/μm). (Figure appears in color online.)

bin is then plotted as a function of the azimuthal angle,  $\beta$ , from the applied field direction as shown in Figure 9.

The orientational order parameter for the distribution of lattice plane normals ( $P_{2,r}$ ) can then be determined using (Eq. (2)).

$$\overline{P_{2,z}} = \frac{1}{z} \int_0^{180} I(\beta) \left( \frac{3}{2} \cos^2 \beta - \frac{1}{2} \right) \sin \beta d\beta \quad \text{where, } z = \int_0^{180} I(\beta) \sin \beta d\beta \quad (2)$$

and  $I(\beta)$  is the Bragg intensity distribution. As the scattering from the lattice planes aligns perpendicular to the electric field this generates an order parameter tending to  $-1/2$  for perfect alignment and 0 for isotropic.

To follow the effect of electric field on particle orientational order, it was necessary to develop an empirical figure of merit. This represents the degree of alignment indicated by the particle form scattering which was gathered using the long camera length. This involved taking an intensity ratio for a vertical band against a horizontal band (Fig. 10).

An isotropic sample has a ratio of 1 and as the scattering becomes more extended the intensity ratio increases. The intensity ratio is  $Q$  dependent so its value at  $Q = 0.02 \text{ \AA}^{-1}$  where it tended to be largest has been used. To follow the intensity ratio variation with field, a plot of the ratio vs field is generated.

### 3. Results and Discussion

It was found that at all concentrations the order parameter determined from the Bragg peak decreased monotonically with field and no threshold effects were observed (Fig. 11(a)).



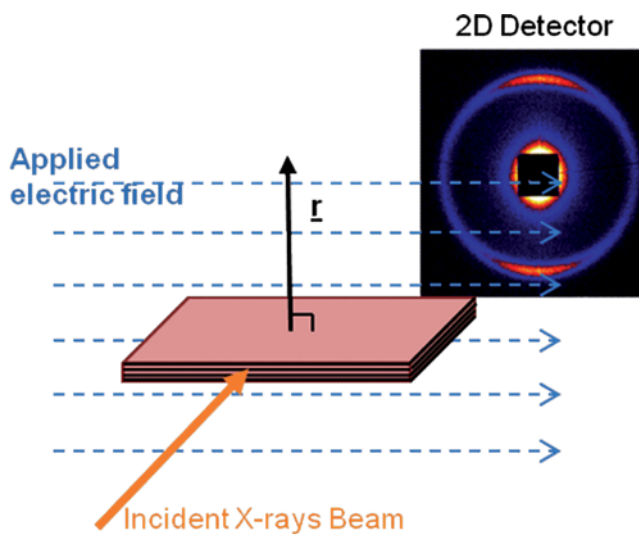


**Figure 8.** Schematic diagram showing the orientation of the platelets and lattice planes with applied electric field. (Figure appears in color online.)

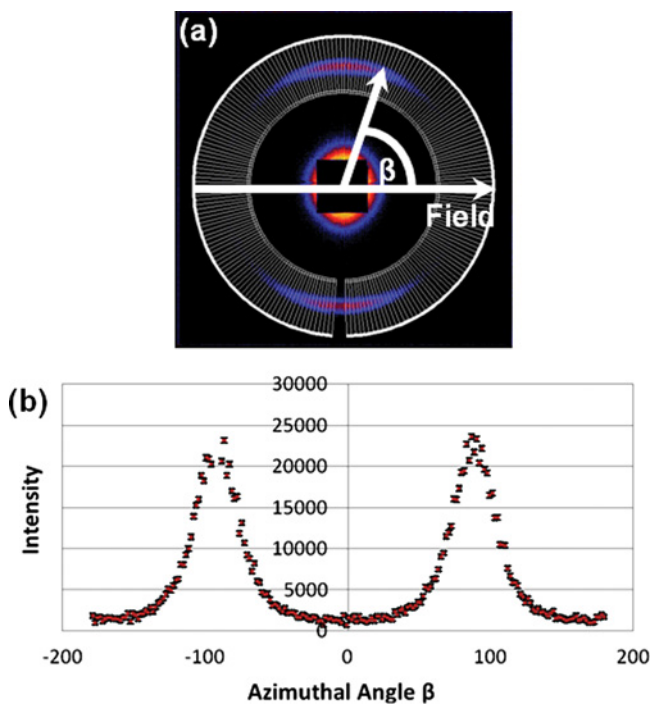


**Figure 9.** (a) Scattering pattern obtained using short camera length for 25 wt% Permanent Rubine in dodecane with the field ( $4.25 \text{ V}/\mu\text{m}$ ) direction marked (b) Intensity of Permanent Rubine peak ( $Q = 0.35 \text{ \AA}^{-1}$ ) as a function of azimuthal angle  $\beta$  for  $4.25 \text{ V}/\mu\text{m}$ . (Figure appears in color online.)

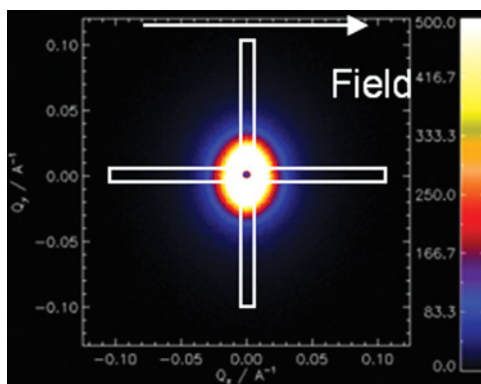


**Figure 10.** Particle form scattering showing bands used to calculate intensity ratio. (Figure appears in color online.)

From Figure 11(b) it can be seen that as the concentration increases from zero there is initially a decrease in order. However there is stronger electro-induced order at 25 wt% and 30 wt% before it drops at 35 wt%. The 35 wt% suspension was initially flow aligned in the sample tube and showed a small response to the applied field which is consistent with its high viscosity. It should be noted that for concentrations of 25 wt% and less, when the applied field was removed the samples did relax to an order parameter of 0 within 20 s (the interval time between experimental runs). For concentrations above 25 wt% the samples still showed some relaxation but they did not return to their original state within a time frame of 90 seconds. More detailed studies of the relaxation dynamics of these systems are planned.

Figure 12(b) shows the intensity ratio increasing with applied field. These results clearly show the same pattern as the order parameter results with all except 35 wt% showing a response to the field. There is also no threshold field observed. As the concentration increases, there is initially a decrease in order with an increase at 25 wt% which is consistent with the order parameter results from the Bragg peak. Comparison of the order parameter from the Bragg peak with the intensity ratio of the particle form scattering confirms the picture of thin flat particles with lattice planes spaced by 18 Å parallel to the large faces and tending to align with the large faces perpendicular to the applied electric field.

The magnitude of the electrically induced absorbance change can be rationalised by the change in orientational order parameter that has been determined by X-rays. A simple model is suggested. If the particle transition dipole moment ( $\mu$ ) is in the plane of the particle and application of a field tends to align the particle normal ( $\mathbf{r}$ ), perpendicular to the field then a decrease in absorption is expected because the transition dipole is less parallel to the electric vector of the light (Fig. 13(a)). To quantify this expectation, it is assumed that self-shielding within the particles is negligible, light scattering is negligible, there is a uniaxial distribution of  $\mathbf{r}$  about the applied field and that the transition dipole moment is isotropically distributed within the plane of each particle.

The proportional change in absorbance may be calculated from the alignment of the transition dipole moment relative to the incident light. The absorbance,  $A$ , is proportional to the mean value of cosine squared of the angle,  $\delta$ , between the transition

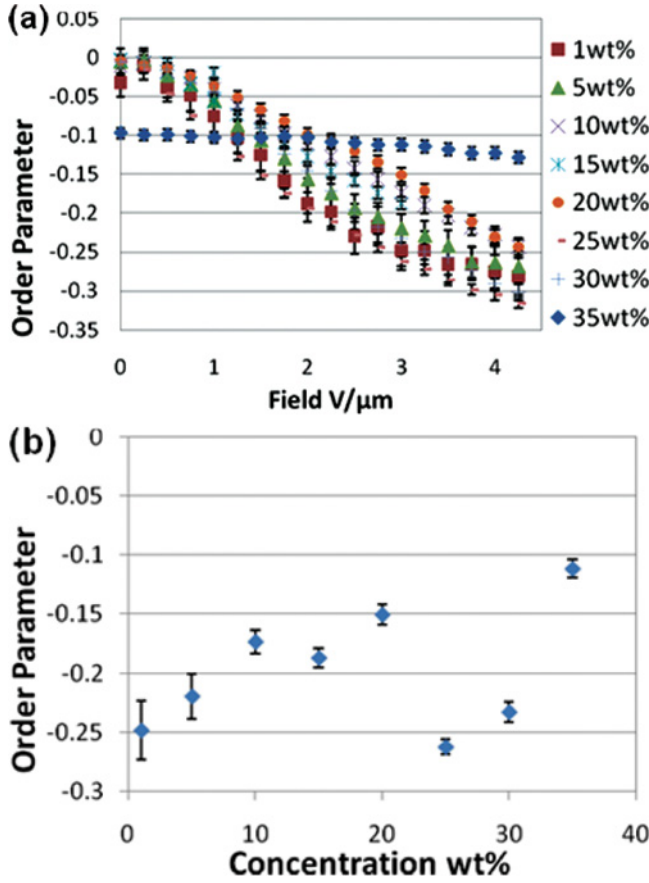


**Figure 11.** (a) A graph of order parameter as a function of applied field for constant concentration. (b) A graph of order parameter as a function of concentration at constant field ( $3 \text{ V}/\mu\text{m}$ ).

dipole moment and the electric vector of the light. This is calculated from the unit vector along the transition dipole moment given by:

$$\hat{\underline{\mu}} = \cos \alpha \cos \beta \underline{i} + \sin \alpha \underline{j} + \cos \alpha \sin \beta \underline{k}, \quad (3)$$

where  $\beta$  is the angle between the platelet normal  $\underline{r}$  and the propagation direction of light as well as applied electric field and  $\alpha$  is the azimuthal angle of the dipole,  $\underline{\mu}$ , within the plane of the particle as shown in Figure 13(b). The plane of polarising incident light is dependent on  $\phi$ :

$$\hat{\underline{E}} = \cos \phi \underline{i} + \sin \phi \underline{j} \quad (4)$$

and taking the dot product of  $\hat{\underline{E}}$  and  $\hat{\underline{\mu}}$  gives the angle  $\delta$ :

$$\cos \delta = \hat{\underline{E}} \cdot \hat{\underline{\mu}} = \cos \alpha \cos \beta \cos \phi + \sin \phi \sin \alpha. \quad (5)$$

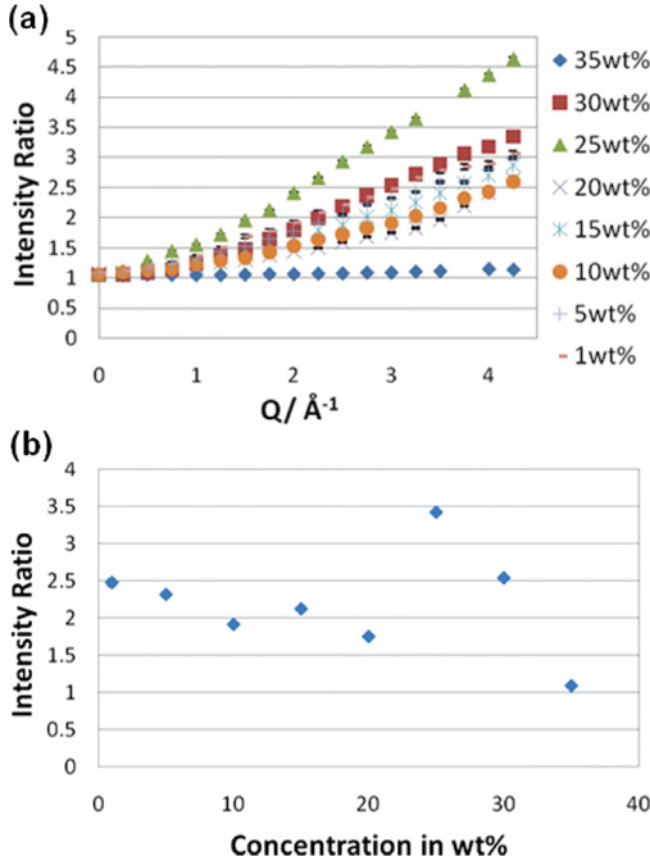


**Figure 12.** (a) A graph of intensity ratio as a function of applied field for  $Q=0.02 \text{ \AA}^{-1}$ . (b) A graph of intensity ratio as a function of concentration at constant field ( $3 \text{ V}/\mu\text{m}$ ).

Then taking the square and averaging over  $\phi$  for un-polarised light and averaging over  $\alpha$  because of the distribution of  $\mu$  within the particle gives:

$$\langle \cos^2 \delta \rangle = \frac{1}{4} \langle \cos^2 \beta \rangle + \frac{1}{4}, \quad (6)$$

which is then combined with the definition of the orientational order parameter:

$$P_{2,z} = \frac{3}{2} \langle \cos^2 \beta \rangle - \frac{1}{2}. \quad (7)$$

This gives the relationship between the absorbance and the order parameter of the lattice plane normals.

$$A \propto \langle \cos^2 \delta \rangle = \left( \frac{P_{2,z} + 2}{6} \right) \quad (8)$$

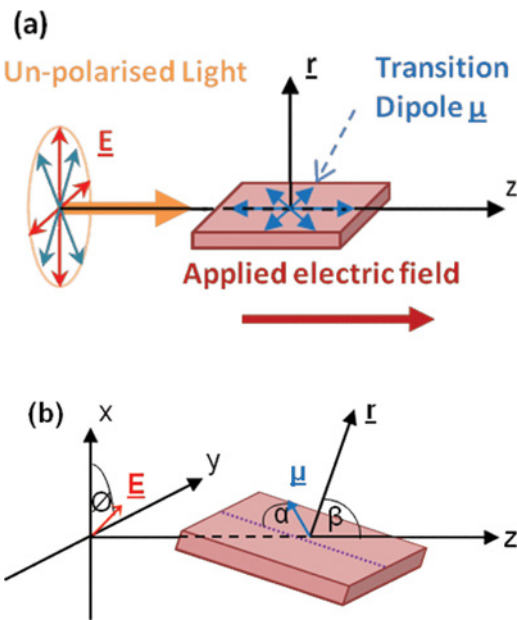


**Figure 13.** Schematic diagram of platelet particle with light propagating in the z direction (a) Showing schematically the transition dipole moment distribution within the plane of the particle and the alignment with applied electric field (b) Showing the angles used to define the orientation of the transition dipole moment ( $\mu$ ) and the electric vector  $\underline{E}$  of the light. (Figure appears in color online.)

The X-ray order parameter of a 5 wt% sample (Fig. 11(a)) shows a change in  $P_{2,x}$  from 0 to  $-0.28$  when a field of  $4.25 \text{ V}/\mu\text{m}$  is applied. For this change, the above formula predicts a decrease in absorbance by a factor of 0.86 which is consistent with the factor of 0.82 observed in Figure 3(b).

The neglect of self shielding does require justification. In particle suspensions, the Beer-Lambert law is only valid in the limit of low attenuation coefficient of

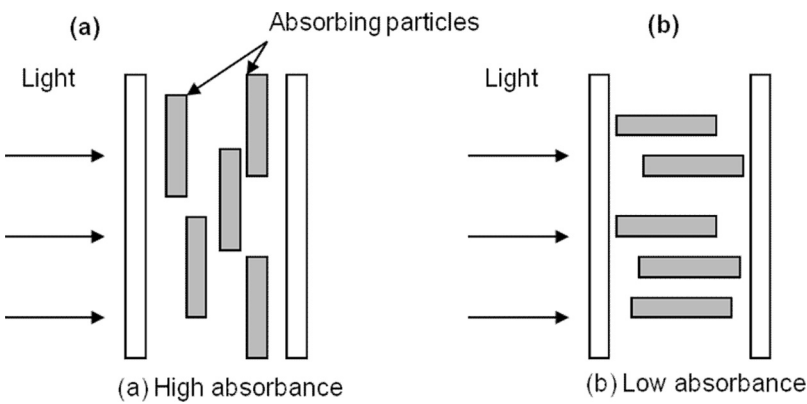


**Figure 14.** Showing schematically the effect of particle dimension in the direction of light propagation on absorbance. In (a) all the rays are blocked by particles but in (b) a fraction of the rays will pass through the solvent.

the particles. For strongly attenuating particles, the dimension of the particle in the direction of light propagation is important. If this dimension is small, the particle area presented to the incoming photon is large and so there is a high probability of it hitting a particle and being absorbed (Fig. 14(a)). However, if the dimension is large, the area presented is small and so there is a low probability of absorption (Fig. 14(b)). Thus it is possible that turning the platelet particles around so that their long dimension is parallel to the light could produce a decrease in absorbance.

A more detailed analysis of this effect will be published separately but it appears not to be a major factor in the effect observed here. The reason is that the display dichroic ratio is the same, within experimental error, when measured at 570 nm and at 400–490 nm. If self shielding were important, it would contribute strongly to the value at 570 nm where the absorptivity is high and less at 400–490 nm so the dichroic ratios would be different.

#### 4. Conclusion

It has been shown that a suspension of highly polydisperse anisometric dye particles in a simple liquid solvent such as dodecane can give a suspension with nematic like properties such as Schlieren texture and an electro-optic response. The thin plate-like particles of the Permanent Rubine are good crystalline monodomains with a set of 18 Å lattice planes lying parallel to their largest faces. They can be oriented by an electric field such that their normals tend to be perpendicular to the applied field. The stronger ordering at about 25 wt% suggest that this might be the onset of the nematic phase and that the suspensions remain nematic beyond 35 wt% but are too viscous to respond to the field in a reasonable time scale. The change in optical absorbance with the application of field is consistent with the induced orientational order.

There is clearly considerable scope for developing such systems. It is planned to improve the polydispersity and to explore different shaped particles in future.

#### Acknowledgment

We are grateful for the financial support of an Open Innovation Research Award from Hewlett Packard.

#### References

- [1] van der Kooij, F. M., & Lekkerkerker, H. N. W. (1998). *The Journal of Physical Chemistry B*, 102, 7829.
- [2] van der Beek, D., Davidson, P., & Wensink, H. H., *et al.* (2008). *Phys. Rev. E Stat Nonlin Soft Matter Phys.*, 77, 031708.
- [3] van der Beek, D., Petukhov, A. V., & Davidson, P., *et al.* (2006). *Phys. Rev. E*, 73, 041402.
- [4] (1971). Colour index. In: *Society of Dyers and Colourists*, Bradford, 3rd Edition, 3308.
- [5] <http://www.diamond.ac.uk/Home/Beamlines/I22.html>.
- [6] Connolly, J., van Duijneveldt, J. S., & Klein, S., *et al.* (2007). *Journal of Physics-Condensed Matter*, 19.
- [7] Purdy, K. R., Dogic, Z., & Fraden, S., *et al.* (2003). *Phys. Rev. E*, 67, 031708.
- [8] Oldenbourg, R., Wen, X., & Meyer, R. B., *et al.* (1988). *Phys. Rev. Lett.*, 61, 1851.
- [9] Clarke, S. M., Rennie, A. R., & Convert, P. (1996). *Europhys. Lett.*, 35, 233.
- [10] Scherrer, J. (1918). *Göttinger Nachrichten*.